

FEM simulation of unsteady viscous incompressible fluid flows

A. Tralli*, P. Gaudenzi

Dipartimento di Ingegneria Aerospaziale e Astronautica, Università di Roma 'La Sapienza', Via Eudossiana, 16, Rome, Italy

Abstract

A fractional-step method to solve unsteady viscous incompressible flows is described. A semi-implicit time-advancement scheme is used to solve the dynamics equations, and the space discretization is performed by Finite Elements. The 2-D flow in a driven cavity at $Re = 1000$ and around a cylinder at $Re = 100$ are presented, with good correspondence with the benchmark solutions.

Keywords: Fractional step; FEM; Incompressible; Viscous flow; Unsteady; Driven cavity; Cylinder

1. Introduction

The present work shows the solution of some benchmark cases involving unsteady flow of an incompressible viscous fluid, obtained by a fractional-step algorithm, in conjunction with a Finite Elements Method (FEM) space discretization. The FEM is gaining more and more importance in computational fluid dynamics, due to its strong mathematical foundation and the capability to deal with complex geometries and heavy mesh grading.

Fractional-step methods are a wide class of solution strategies to account for the incompressibility constraint. Introduced by Chorin [1,2] and, independently, Temam [3], they are probably the most widely used methods to integrate the incompressible Navier-Stokes equations.

Many numerical codes have been developed in conjunction with space discretizations obtained by Finite Differences (see, for example, Orlandi [4] and references therein, Kim et al. [5], Rai et al. [6], and Verzicco et al. [7]). Fractional-step methods are often coupled also with Spectral Elements [8], and with Finite Elements, using an inexact block-factorization of the complete algebraic system [9,10] or a projection method at a differential level, as in [11] and in the present procedure, described in detail in [12].

2. Navier-Stokes equations

The solution of the governing equations of fluid dynamics consists in finding a velocity vector field $\mathbf{u}_{(x,t)}$ and a pressure $p_{(x,t)}$ satisfying, in a Cartesian reference frame $(x_i, i = 1, 2, 3)$, the equilibrium

$$\rho \dot{u}_i + (\rho u_i u_j - \tau_{ij})_{,j} = g_i \quad (1)$$

and the continuity equation:

$$u_{i,i} = 0 \quad (2)$$

for $(\mathbf{x}, t) \in \Omega \times [0, T]$ where ρ is the (constant and uniform) fluid density, g_i accounts for the body forces (assumed constant in the following), and the time derivatives are indicated by a dot. A Newtonian rheology is considered,

$$\tau_{ij} = -p\delta_{ij} + \mu(u_{i,j} + u_{j,i}) = -p\delta_{ij} + 2\mu e_{ij} \quad (3)$$

where μ is the dynamic viscosity and $e_{ij} = \frac{1}{2}(u_{i,j} + u_{j,i})$ is a component of the strain rate tensor. NS equations are subject to initial and boundary conditions

$$u_{i(x,0)} = u_{i(x)}^0, \quad \mathbf{x} \in \Omega \quad (4)$$

$$u_{i(x,t)} = u_{i(x,t)}^b, \quad \mathbf{x} \in \partial\Omega^b \quad (5)$$

$$\tau_{ij(x,t)} n_j = f_{i(x,t)}^F, \quad (\mathbf{x}, t) \in \partial\Omega^F \times [0, T] \quad (6)$$

3. Solution procedure

We briefly outline the logics followed to obtain the

* Corresponding author. Tel.: +39 (0) 644 585738; Fax: +39 (0) 644 585670; E-mail: aldo.tralli@uniroma1.it

discrete governing equations: Eq. (1) is discretized in time by a semi-implicit algorithm: non-linear terms are treated explicitly (III-order Runge Kutta, RK), and linear terms, namely the viscous and the pressure term, are treated implicitly (Crank-Nicholson, CN). The k -th of three steps is split into two substeps: the first substep reads

$$\frac{\rho}{\Delta t} \left({}^{(k)}u_i^* - {}^{(k-1)}u_i \right) + \gamma_k \rho^{(k-1)} N_i + \lambda_k \rho^{(k-2)} N_{i,j} \\ = {}^{(k)}g_i - \alpha_k {}^{(k-1)}p_{,i} + \frac{\alpha_k}{2} \left(2\mu^{(k)} e_{ij}^* + 2\mu^{(k-1)} e_{ij,j} \right) \quad (7)$$

where ${}^{(k)}u_i^*$ is a non-solenoidal, intermediate velocity field, satisfying the equilibrium, subject to the boundary conditions on the end-of-step velocity ${}^{(k)}u_i$; the convective term ${}^{(k)}N_i = ({}^{(k)}u_i {}^{(k)}u_j)$ is solved in conservative form, e_{ij}^* is calculated from u_i^* . The coefficients γ_n , α_n , λ_n are calculated as in [4].

It is possible (from the Helmholtz theorem) to split ${}^{(k)}u_i^*$ into the sum of a solenoidal and an irrotational field,

$${}^{(k)}u_i^* = {}^{(k)}u_i + {}^{(k)}\phi_{,i} \quad (8)$$

where ${}^{(k)}u_i$ is the sought end-of-step velocity, and ϕ is a scalar field. Taking the divergence of Eq. (8) and enforcing incompressibility, e.g. ${}^{(k)}u_{i,i} = 0$, we obtain

$${}^{(k)}u_{i,i}^* = {}^{(k)}\phi_{,ii} \quad (9)$$

In the code, Eq. (9) is modified to

$$\left({}^{(k)}u_i^* - {}^{(k-1)}u_i \right)_{,i} = {}^{(k)}\phi_{,ii} \quad (10)$$

which is the second substep, complemented with homogeneous natural b.c. on ${}^{(k)}\phi$ (actually, essential b.c. must be enforced in one point, to get a unique ${}^{(k)}\phi$): the scalar field ${}^{(k)}\phi$, is used in Eq. (8) to get the new, divergence-free velocity ${}^{(k)}u_i$.

Also the new pressure gradient is obtained, requiring a second-order (CN) approximation in time also for that term

$${}^{(k)}p_{,i} = \frac{{}^{(k-1)}p_{,i}}{2} + \frac{\rho}{\alpha_i \Delta t} {}^{(k)}\phi_{,i} - \mu \left({}^{(k)}\phi_{,ijj} + {}^{(k)}\phi_{,ijj} \right) \quad (11)$$

To avoid the calculation of the third derivatives of ${}^{(k)}\phi$, we modify Eq. (7) to

$$\frac{\rho}{\Delta t} \left({}^{(k)}u_i^* - {}^{(k-1)}u_i \right) + \gamma_k \rho^{(k-1)} N_{i,j} + \lambda_k \rho^{(k-2)} N_i, \\ = {}^{(k)}g_i - \alpha_k {}^{(k-1)}\tilde{p}_{,i} + \frac{\alpha_k}{2} \left(2\mu^{(k)} e_{ij}^* + 2\mu^{(k-1)} e_{ij,j}^* \right) \quad (12)$$

using ${}^{(k)}\tilde{p}_{,i} = \frac{{}^{(k-1)}\tilde{p}_{,i}}{2} + \frac{\rho}{\alpha_i \Delta t} {}^{(k)}\phi_{,i}$; the correct value for the pressure is calculated in the post-processing.

The discrete equations are obtained by subdividing Ω into N subdomains Ω_n , $n = 1, 2 \dots N$ and establishing a

weak form of Eqs. (12) and (13) using the Galerkin procedure: Eq. (12) is weighted with the velocities,

$$\int_{\Omega_n} \hat{u}_i \rho^{(k)} u_i^* d\Omega + \int_{\Omega_n} \hat{e}_{ij} \frac{\alpha_k \Delta t}{2} 2\mu^{(k)} e_{ij}^* d\Omega = \\ \int_{\Omega_n} \hat{u}_i \rho^{(k-1)} u_i d\Omega + \\ + \int_{\Omega_n} \Delta t \hat{u}_i {}^{(k)}g_i d\Omega + \int_{\partial\Omega_n^F} \hat{u}_i \frac{\alpha_k \Delta t^{(k-1)}}{2} f_i^F ds + \\ \int_{\partial\Omega_n^F} \hat{u}_i \frac{\alpha_k \Delta t^{(k)}}{2} f_i^F ds + \\ - \int_{\Omega_n} \hat{u}_i \gamma_k \Delta t \rho^{(k-1)} N_i d\Omega - \int_{\Omega_n} \hat{u}_i \lambda_k \Delta t \rho^{(k-2)} N_i d\Omega + \\ \int_{\Omega_n} \hat{e}_{ij} \alpha_k \Delta t^{(k-1)} \tilde{p} \delta_{ij} d\Omega - \int_{\Omega_n} \hat{e}_{ij} \frac{\alpha_k \Delta t^{(k-1)}}{2} 2\mu e_{ij}^* d\Omega \quad (13)$$

Equation (14) is weighted with the scalar ϕ :

$$\int_{\Omega_n} \hat{\phi}_{,i} {}^{(k)}\phi_{,i} d\Omega = \int_{\Omega_n} \hat{\phi} \left({}^{(k)}u_i^* - {}^{(k-1)}u_i \right)_{,i} d\Omega \\ + \int_{\partial\Omega_n} \hat{\phi} {}^{(k)}\phi_{,i} n_i ds \quad (14)$$

the hat denotes weighting quantities. The divergence theorem has been applied in Eqs. (13) and (14), in order to lower the derivation order and to account for the natural boundary conditions, as in [12].

The resulting, assembled discrete equations are

$$\left([M] + \Delta t \frac{\alpha_k}{2} [K] \right) {}^{(k)}\{u\}^* = [M] {}^{(k-1)}\{u\} \\ + \Delta t \gamma_k {}^{(k-1)}\{N\} - \Delta t \lambda_k {}^{(k-2)}\{N\} \\ + \Delta t \frac{\alpha_k}{2} \left(2 {}^{(k-1)}\{\hat{D}_p\} + [K] {}^{(k-1)}\{\hat{u}\}^* \right) + {}^{(k)}\{R\} \quad (15.a)$$

$${}^{(k)}\{D\}^* = [L] {}^{(k)}\{\phi\} \quad (15.b)$$

$${}^{(k)}\{u\} = {}^{(k)}\{u\}^* - {}^{(k)}\{\phi_{,i}\} \quad (15.c)$$

where ${}^{(k)}\{u\}$ is the vector of the nodal velocity components, $[M]$ and $[K]$ are the consistent mass and viscous matrix, respectively; ${}^{(k)}\{N\}$ accounts for the convective term, calculated from the velocity at the previous step; ${}^{(k-1)}\{\hat{D}_p\}$ and ${}^{(k)}\{D\}^*$ are the FEM counterpart of $-{}^{(k-1)}\tilde{p}_{,i}$ and ${}^{(k)}u_{i,i}^*$, respectively. ${}^{(k)}\{R\}$ accounts for volume and boundary loads.

$[L]$ is the discrete Laplace operator and ${}^{(k)}\{\phi\}$ is the vector of the nodal values of the scalar field used in the projection. Δt is the selected time step.

Once the scalar field ${}^{(k)}\{\phi\}$ has been calculated, it is to

be used to calculate the new, solenoidal velocity vector $^{(k)}\{u\}$, using Eq. (15.c): a continuous estimate of $^{(k)}\{\phi_{,i}\}$ is evaluated, from $^{(k)}\{\phi\}$, by a nodal point average.

Due to the incompressibility constraint, a proper mixed formulation is adopted, using a 9/4-c quadrilateral finite element, described in [13]: bi-quadratic displacement interpolation is used on the velocities, and bi-linear interpolation is used on the pressure and the scalar ϕ , with ϕ (and \bar{p}) continuous across the element's edge. This element satisfies the *inf-sup* condition, and is expected to guarantee acceptable accuracy on distorted grids, at least for the velocity.

The skyline solver *COLSOL*, documented in [13], is used to solve Eqs. (15.a,b). The pre-processing operations, namely the geometrical set-up, the space discretization, and the equation numbering optimization, are performed through the commercial code ADINA-AUI 8.0.

4. Numerical examples

4.1. Start-up of a driven cavity

The flow in a square domain is simulated: no-slip boundary conditions are assigned on three edges and a tangential velocity component imposed on the fourth, upper edge. The domain is subdivided into 48×48 elements (9409 nodes); the transient following a sudden start of the upper wall is simulated, at $Re = 1000$, using a time step $\Delta t = 0.01$ s. Fig. 1 shows the streamlines pattern at $t = 5$ s and at $t = 100$ s. In Fig. 2 the velocity profiles are compared with results in [14].

4.2. Flow around a cylinder

The 2-D flow around a cylinder at $Re = 100$ is simulated: the computational domain is represented in Fig. 3; unit horizontal velocity is imposed at the (semi-circular) inflow, zero normal velocity and zero tangential stress are assumed at the lateral boundaries, and a traction-free condition and zero tangential velocity are prescribed at the outflow boundary. The simulation, with $\Delta t = 0.005$ s, begins with an impulsive start of the cylinder: a divergence-free initial velocity field is obtained by calculating Eqs. (18.b,c) on a uniform, unit velocity field on the whole domain. Once a fully periodic solution is obtained, the Strouhal number $S = 0.165$ is calculated, which is in satisfactory agreement with experimental results in the literature [15]. Fig. 4 reproduces the contour plot of the vertical velocity component at $t = 150$ s.

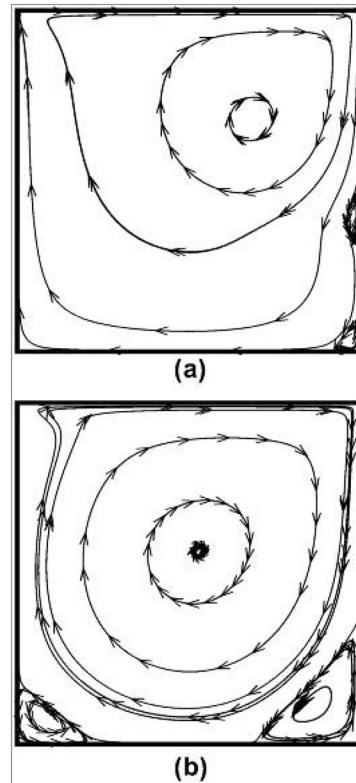


Fig. 1. Driven cavity, $Re = 1000$ – streamlines pattern: (a) $t = 5$ s, (b) $t = 100$ s.

5. Conclusions

A simple and robust algorithm for the direct simulation of incompressible fluid flows is described. Testing of the procedure on a range of benchmark cases is under way, but the preliminary results shown in this paper are very promising. The fractional-step technique used is robust and very fast, and is suitable for extension to 3-D computations. In the future, numerical tests will be performed, to assess the accuracy, in space and time, for both the velocity and pressure field.

References

- [1] Chorin AJ. Numerical solution of the Navier–Stokes equations. *Math Comput* 1968;22:745–762.
- [2] Chorin AJ. On the convergence of discrete approximations to the Navier–Stokes equations. *Math Comput* 1969;23:341–353.
- [3] Temam R. Sur l’approximation de la solution des équations de Navier–Stokes par la méthode des pas fractionnaires. II. *Arch Rational Mech Anal* 1969;33:377–385.

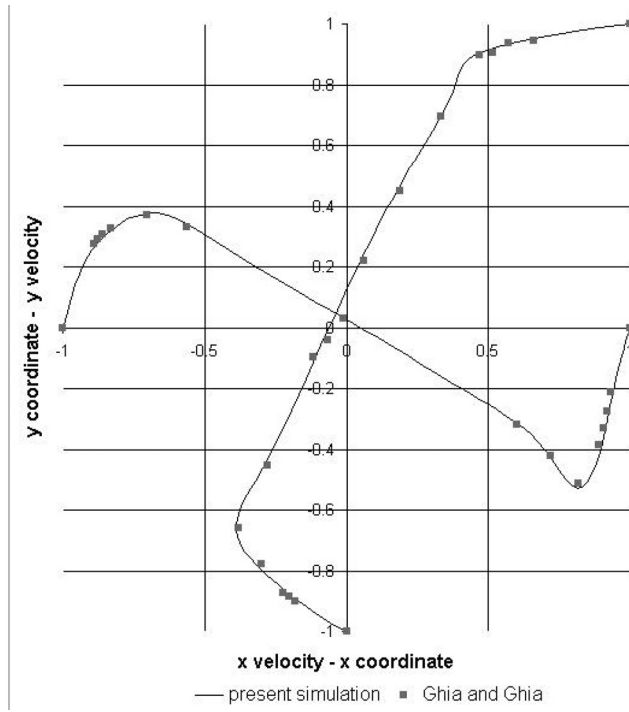


Fig. 2. Driven cavity: $Re = 1000$ – steady centreline velocities: comparison with [14].

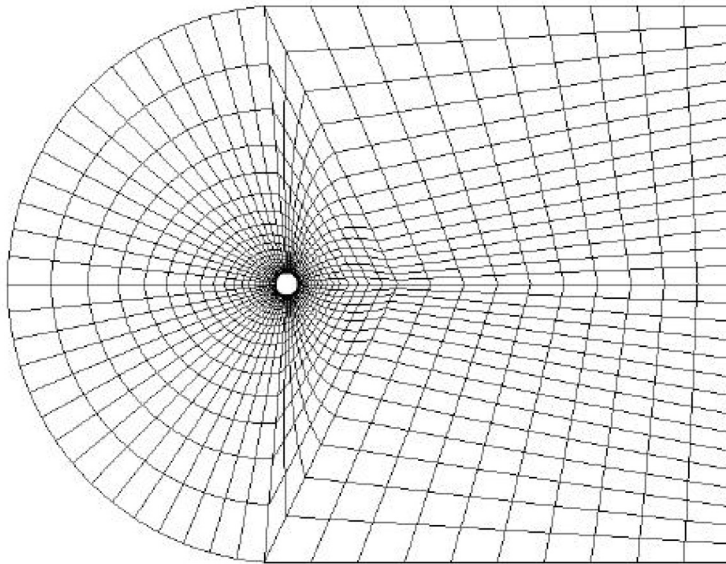


Fig. 3. Flow around a cylinder – geometry and mesh (6140 nodes).

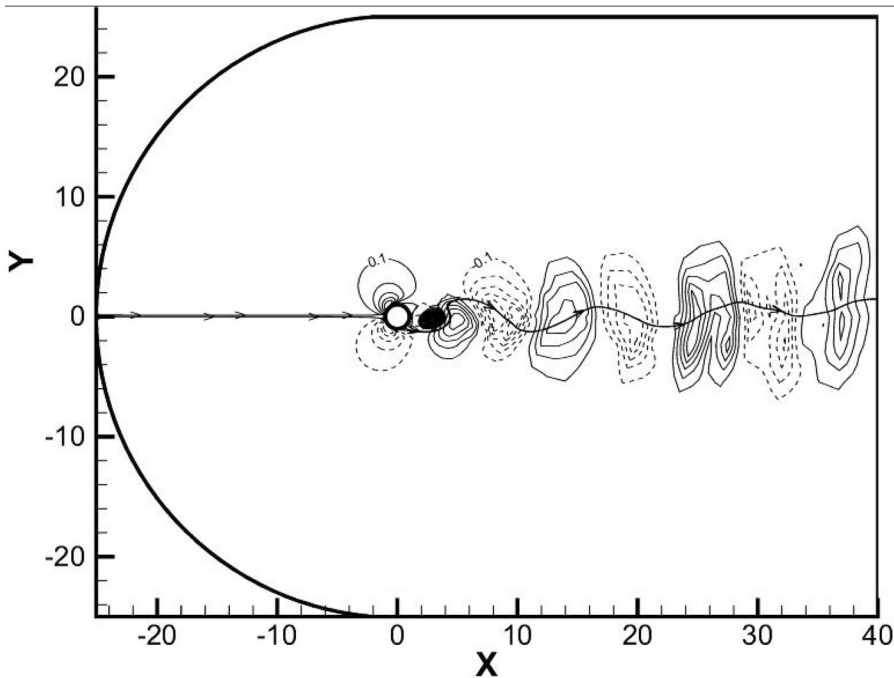


Fig. 4. Flow around a cylinder, $Re = 100$ – streamlines, y velocity contours, $\delta = 0.1$.

- [4] Orlandi P. *Fluid Flow Phenomena: A Numerical Toolkit*. Kluwer Academic Publishers, 1999.
- [5] Kim J, Moin P. Application of a fractional-step method to incompressible Navier–Stokes equations. *J Comput Phys* 1985;59:308–323.
- [6] Rai M, Moin P. Direct simulation of turbulent flow using finite difference schemes. *J Comput Phys* 1991;96:15–53.
- [7] Verzicco R, Orlandi P. A finite-difference scheme for three-dimensional incompressible flows in cylindrical coordinates. *J Comput Phys* 1996;123:402–414.
- [8] Timmermans LJP, Mineev PD, Van De Vosse FN. An approximate projection scheme for incompressible flow using spectral elements. *Int J Numer Methods Fluids* 1996;22:1719–1737.
- [9] Quarteroni A, Saleri F, Veneziani A. Analysis of the Yosida method for the incompressible Navier–Stokes equations. *J Math Pure Appl* 1999;78:473–503.
- [10] Perot B. An analysis of the fractional step method. *J Comput Phys* 1993;108:51–58.
- [11] Guermond JL, Quartapelle L. Calculation of incompressible viscous flows by an unconditionally stable projection FEM. *J Comput Phys* 1997;132:12–33.
- [12] Tralli A, Gaudenzi P. Simulation of unsteady incompressible flows by a fractional step FEM. Submitted to *Int J of Numer Models in Eng*.
- [13] Bathe KJ. *Finite Element Procedures*. Englewood Cliffs: Prentice-Hall, 1995.
- [14] Ghia U, Ghia KN, Shin CT. High-Re solutions for incompressible flow using the Navier–Stokes equations and a multigrid method. *J Comput Phys* 1982;48:387–411.
- [15] Williamson CHK. Oblique and parallel modes of vortex shedding in the wake of a circular cylinder at low Reynolds numbers. *J Fluid Mech* 1989;206:203–213.